Nontemplated Nucleotide Addition by HIV-1 Reverse Transcriptase[†]

Marie-Pierre Golinelli[‡] and Stephen H. Hughes*

HIV Drug Resistance Program, National Cancer Institute at Frederick, P.O. Box B, Building 539, Room 130A, Frederick, Maryland 21702-1201

Received December 18, 2001; Revised Manuscript Received March 12, 2002

ABSTRACT: We studied the kinetics of nontemplated nucleotide addition by the reverse transcriptase (RT) of human immunodeficiency virus type 1 (HIV-1) using model substrates derived from the 3′ end of HIV-1 minus-strand strong-stop DNA. The addition of a nontemplated nucleotide was highly dependent on the nature of the base (fastest addition with dATP), type of nucleoside, and pH of the reaction buffer. The salt concentration, presence or absence of nucleocapsid protein, and nature of the blunt-ended duplex (DNA/DNA versus RNA/DNA) had only limited effects. The efficiency and base specificity were strongly affected by the sequence at the 3′ end of the blunt-ended duplex. In every case, nontemplated nucleotide addition was much slower than templated polymerization. The K_d for the incoming dNTP with an RT bound to a blunt-ended duplex was at least 1000-fold higher than with a duplex with a template overhang. At concentrations normally found in vivo, ATP can compete with dNTPs for binding to the polymerase active site and reduce the efficiency of nontemplated nucleotide addition. Although a stable ternary complex RT/DNA/dNTP could be readily detected by gel retardation assays if the DNA had a template overhang, stable ternary complexes were not observed with a blunt-ended duplex substrate. At in vivo concentrations of dNTPs (5−10 μM), nontemplated nucleotide addition occurred, but it was very inefficient and the rate of nontemplated polymerization is at least 10000-fold slower than the rate of templated polymerization. We could conclude that, in vivo, the unfavorable binding of the incoming dNTP, low concentration of dNTPs, the presence of a large concentration of ATP, and the inability to form a stable ternary complex prior to the polymerization step collaborate to reduce the efficiency of nontemplated nucleotide addition.

Retroviral reverse transcriptases (RTs)[1] synthesize viral minus-strand DNA using the RNA genome as a template and plus-strand DNA using minus-strand DNA as a template. DNA synthesis is initiated from a primer tRNA bound to the primer-binding site (PBS) (*1*−*3*); the U5 and R regions at the 5′ end of the RNA genome are the first to be copied. The RNase H activity of RT degrades the RNA strand after it has been copied (*4*−*6*). When RT reaches the 5′ end of the genomic RNA, the nascent single-stranded DNA (ssDNA), which is called minus-strand strong-stop DNA (−sssDNA), is transferred to the R region at the 3′ end of the RNA genome and the synthesis of minus-strand DNA continues (*7*−*9*).

Using ssDNA models whose sequences are complementary to the R region of the genomic RNA (−R ssDNA) of human immunodeficiency virus type 1 (HIV-1), human immunodeficiency virus type 2 (HIV-2), and human T cell leukemia virus type 1 (HTLV-1), we showed that these −R ssDNAs could self-prime in vitro and that self-priming could be prevented by annealing a DNA oligonucleotide to the 3′ end of −R ssDNA in the presence or absence of the HIV-1 nucleocapsid protein (NC) (*10*, *11*). However, when such DNA oligonucleotides were added in large excess, one-base-pair strand transfer could be induced in vitro (*12*).

Using HIV-2 −R ssDNA as a model, we previously demonstrated that nonspecific strand transfer was induced by the addition of a nontemplated dA or dC to the 3′ end of the blunt-ended duplex formed by a 20-mer DNA oligonucleotide annealed to the 3′ end of HIV-2 −R ssDNA (*12*). Strand transfer required the formation of at least one canonical Watson−Crick base pair between the nontemplated nucleotide added at the 3′ end of the duplex and the last base at the 3′ end of the ssDNA acceptor. Formation of mispairs or internal base pairs did not induce efficient one-base-pair strand transfer. We proposed that such one-base-pair strand transfer could explain some of the insertions and deletions observed in retroviral genomes (*12*). Similar nontemplated nucleotide addition/one-base-pair strand transfer reactions were also observed in vitro with other −R ssDNA sequences, e.g., HIV-1 and HTLV-1 −R ssDNA, and with other RTs, e.g., HIV-2 RT and SuperScript II RNase H$^-$ RT (a Moloney murine leukemia virus RNase H$^-$ RT) (*11*, *12*).

[†] Research sponsored by the National Cancer Institute and by the National Institute of General Medical Sciences.

* To whom correspondence may be addressed. Phone: (301) 846-1619. Fax: (301) 846-6966. E-mail: hughes@ncifcrf.gov.

[‡] Present address: Laboratoire d'Enzymologie et de Biologie Structurales, CNRS, 1 Ave. de la Terrasse, 91198 Gif-sur-Yvette, France.

[1] Abbreviations: BSA, bovine serum albumin; DTT, dithiothreitol; EDTA, ethylenediaminetetraacetic acid; HIV-1, human immunodeficiency virus type 1; HIV-2, human immunodeficiency virus type 2; HTLV-1, human T cell leukemia virus type 1; MTO, multiple turnover; NC, nucleocapsid protein; PBS, primer-binding site; −R ssDNA, DNA molecule complementary to the sequence of the R region of a genomic RNA; RT, reverse transcriptase; SDS, sodium dodecyl sulfate; ssDNA, single-stranded DNA; −sssDNA, minus-strand strong-stop DNA; STO, single turnover; TBE, Tris−borate−EDTA; Tris, tris(hydroxymethyl)-aminomethane.

10.1021/bi0160415
Published on Web 04/16/2002

The efficiency of the nontemplated nucleotide addition and the one-base-pair strand transfer seemed to be dependent on the sequence of the 3′ end of the blunt-ended duplex (*12*). Thus, both reactions were less efficient with HIV-1 −R ssDNA than with HIV-2 −R ssDNA. If reactions of this type occur in vivo with an efficiency similar to what we had observed in vitro, we would expect a large number of point mutations, deletions, and/or insertions of nonspecific sequences in retroviral genomes. However, even if some of the errors that arise in retroviral genomes can be attributed to nontemplated nucleotide addition and one-base-pair strand transfer reaction, these events are much rarer in vivo than what we have observed in vitro (*12*). How can we reconcile the in vitro and the in vivo data?

In a previous study (*12*), we reported that HIV-1 NC does not prevent nontemplated nucleotide addition in vitro but can reduce the efficiency of one-base-pair strand transfer in vitro. NC might also reduce the amount of one-base-pair strand transfer in vivo. In the present report, we measured the kinetics of nontemplated nucleotide addition by HIV-1 RT and found that the addition of a nontemplated nucleotide was highly dependent on the nature of the base and the type of nucleoside (the addition of ribonucleosides and dideoxynucleosides was less efficient than deoxynucleosides). With a blunt-ended duplex substrate whose sequence was similar to the 3′ end of HIV-1 −sssDNA, dATP was preferentially added to the end of the DNA whereas dCTP and dTTP were incorporated much less efficiently. The apparent rate of nontemplated nucleotide addition was much slower than templated polymerization even when the dNTP concentration was 500 μM. This difference was due, at least in part, to a much larger K_d for dNTP for nontemplated nucleotide addition (greater than 2 mM) compared to templated nucleotide addition (typically 5−10 μM). Moreover, when reactions were performed in the presence of 10 μM dATP and 3 mM ATP (typical in vivo concentrations for dATP and ATP), the addition of the nontemplated nucleotide was reduced relative to reactions performed in the absence of ATP. Ternary complexes that contain HIV-1 RT/DNA duplex/dNTP are sufficiently stable that they can be observed in a gel retardation assay when the DNA duplex has a template overhang (*13*, *14*). However, in the present study we found that the corresponding complex with a blunt-ended DNA duplex as substrate was not stable enough to be observed by a gel retardation assay. Thus, with a blunt-ended duplex, the ternary complex was considerably less stable than with a template overhang. The stability of the binary complex was also reduced by the absence of a template overhang, showing that a template overhang helps to stabilize both binary and ternary complexes.

At an in vivo concentration of dNTPs (5−10 μM), nontemplated nucleotide addition occurred but was very inefficient, and the rate of nontemplated polymerization was at least 10000-fold slower than the rate of templated polymerization. When a blunt-ended duplex was formed during reverse transcription, nontemplated nucleotide addition competed with the strand transfer of the DNA primer to an homologous template. Nontemplated nucleotide addition was much slower than the strand transfer reaction. The sequence of the 3′ end of the blunt-ended duplex and the pH of the reaction buffer affected both the apparent rate of the nontemplated polymerization and which nucleotide was preferentially added. The salt concentration, presence or absence of NC protein, and nature of the blunt-ended duplex (DNA/DNA versus RNA/DNA) have much more limited effects on the addition of a nontemplated nucleotide. On the basis of these in vitro results, we expect, in vivo, that the unfavorable binding of the incoming dNTP, relatively low concentration of dNTPs, presence of a large concentration of ATP, inability to form stable binary and ternary complexes, and competition with the strand transfer reaction will act together to severely limit nontemplated nucleotide addition to the 3′ end of blunt-ended duplexes.

MATERIALS AND METHODS

HIV-1 RT and Oligonucleotides. Wild-type HIV-1 RT (p66/p51) was expressed in *Escherichia coli* and purified as described previously (*15*). HIV-1 NC (p7 Zn^{2+} NC) was generously provided by Drs. Robert Gorelick, Louis Henderson, and Larry Arthur (SAIC−Frederick). A 30 μM NC solution was prepared by dissolving lyophilized NC in RT binding buffer [50 mM Tris-HCl, pH 8.3, 80 mM KCl, 1 mM dithiothreitol (DTT), 0.1 mg/mL bovine serum albumin (BSA)] containing 20% glycerol. NC was stored in 4 μL aliquots in 150 μL tubes at −80 °C. Fresh aliquots were thawed immediately prior to use.

DNA oligonucleotides were purchased from Invitrogen/Life Technologies and BioSource International, Inc. RNA oligonucleotides (except HIV-1 R RNA) were purchased from Oligos, Etc. HIV-1 R RNA was prepared by in vitro expression as described previously (*10*).

5′ end-labeling of DNA and RNA oligonucleotides was performed using [γ-^{32}P]ATP (Amersham Pharmacia Biotech) and T4 polynucleotide kinase (New England Biolabs). Labeled oligonucleotides were purified on a 12% denaturing polyacrylamide gel. Bands corresponding to the oligonucleotide were cut out, and the oligonucleotides were eluted overnight in water in the presence of proteinase K. After phenol extraction, the oligonucleotide was precipitated, dissolved in TE (10 mM Tris-HCl, pH 7.0, 1 mM EDTA), and quantified by absorption at 260 nm. Gel imaging and quantitation were performed with a Molecular Dynamics Storm 860 PhosphorImager using ImageQuant software version 5.0. Curves were fit using KaleidaGraph software.

DNA and RNA Duplex Substrates. Oligonucleotides with sequences derived from the 5′ end of the HIV-1 RNA genome [GenBank accession number GI328415 (*16*)] were used (Table 1). Duplexes were formed by annealing a template strand (strand B or a modified form of strand B, Table 1) to a 5′ end-labeled primer strand corresponding to the 3′ end of HIV-1 −sssDNA (strand A or a modified form of strand A, Table 1) (Figure 1A). The unlabeled template strand was added in 3-fold excess to the primer strand containing 5−10% of ^{32}P-labeled molecules for kinetic studies and up to 25% for the gel retardation assay. The mixture was incubated at 90 °C for 5 min in RT binding buffer and then was slowly cooled to room temperature.

DNA Secondary Structure Predictions. DNA secondary structure predictions were made using mfold version 3.0 software available on the Zuker and Turner web site (http://bioinfo.math.rpi.edu/~zukerm/export/) (*17*) (J. SantaLucia, Jr., M. Zuker, A. Bommarito, and R. J. Irani, unpublished

Table 1: Sequences Used as Substrates

Strand A (primer)[a]	Strand B (template)[a]
Strand A GCTCAGATCTGGTCTAACCAGAGAGACC	**Strand B** GGTCTCTCTGGTTAGACCAGAGAGC
Strand A Mutant GCTCAGATC<u>A</u>GGTCTAACCAGAGAGACC	**Strand B RNA** GGUCUCUCUGGUUAGACCAGAGAGC
Strand A Short TCTGGTCTAACCAGAGAGACC	**Strand B Pol** **GCAGTG**GGTCTCTCTGGTTAGACCAGAGAGC
Strand A Long **AG**GCTCAGATCTGGTCTAACCAGAGAGACC	**Strand B Mutant** GGTCTCTCTGGTTAGACC<u>T</u>GAGAGC
Strand A 41 mer complementary to bases 1-41 of HIV-1 RNA[b]	**Strand B Long** GGTCTCTCTGGTTAGACCAGA**TCT**GAGC**CTGGGAGCTC**
Strand A+dA GCTCAGATCTGGTCTAACCAGAGAGACC**A**	**Strand B RNA Long** GGUCUCUCUGGUUAGACCAGA**UCU**GAGC**CUGGGAGCUC**
Strand A+dC GCTCAGATCTGGTCTAACCAGAGAGACC**C**	**HIV-1 R RNA** Bases 1 to 100 of HIV-1 RNA genome[b]
Strand A Tail GCTCAGATCTGGTCTAACCAGAGAGACC**AAAAA**	**Strand B Tail** **TTTTT**GGTCTCTCTGGTTAGACCAGAGAGC

[a] Sequence differences between strand A and modified strand A and between strand B and modified strand B are indicated in bold (addition) or are underlined (mutation). [b] HIV-1 genome GenBank accession number GI328415 (*16*).

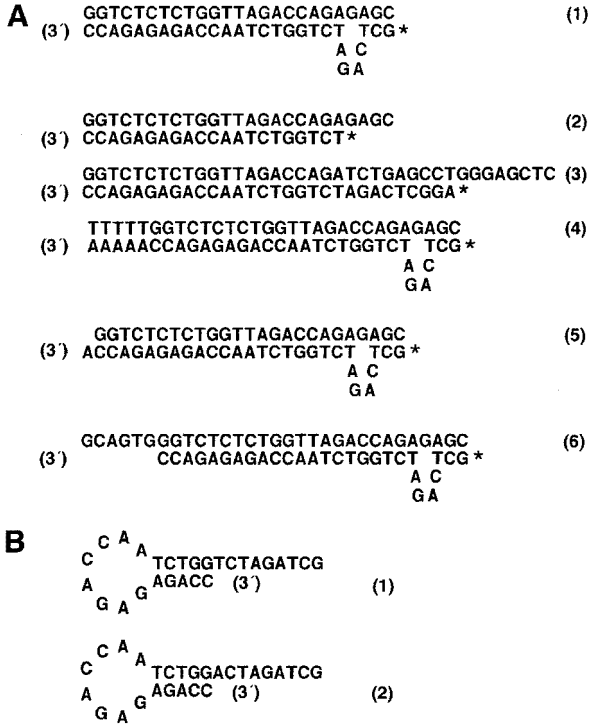

FIGURE 1: Sequences and structures of the nucleic acid substrates used in this study. (A) Sequences of nucleic acid duplexes used in this study: (1) the strand A/strand B duplex; (2) the strand A short/strand B duplex; (3) the strand A long/strand B long duplex; (4) the strand A tail/strand B tail duplex; (5) the strand A + dA/strand B duplex; (6) the strand A/strand B Pol duplex. For all of the sequences, the 5′ end of the primer strand is indicated by an asterisk. (B) The most stable conformation of strand A (1) and strand A mutant (2) with a double-stranded 3′ end ($\Delta G = -2.1$ kcal/mol). Calculations were performed using the SantaLucia algorithm as described in Materials and Methods.

data). Calculations were performed at 37 °C with oligomer corrections and 80 mM NaCl and 6 mM $MgCl_2$, which is equivalent to the salt composition of the buffer used in most of the experiments.

Kinetic Reactions. Nontemplated nucleotide incorporation by HIV-1 RT was investigated by measuring the 3′-terminal extension of a blunt-ended duplex formed by a labeled primer annealed to a template. Typically, 20 nM duplex (assuming that every strand A or modified form of strand A was annealed) was added to a reaction with a final concentration of 200 nM HIV-1 RT, 1 mM fresh DTT, and 1 mM EDTA in RT binding buffer. When an RNA template was used, RNasin RNase inhibitor (Promega) was added to a final concentration of 1 unit/μL. Nucleotide triphosphates [either an NTP (Sigma), a dNTP (Gibco BRL), or a ddNTP (Roche Molecular Systems)] and HIV-1 NC were added as specified. The reactions were preincubated at 37 °C for 5 min and then started by the addition of $MgCl_2$ (6 mM final), which had also been preincubated at 37 °C. Aliquots were removed from the reactions after appropriate incubation and transferred to a tube containing an equal volume of 2× formamide stop solution (90% formamide, 1× TBE, bromophenol blue, and xylene cyanol) containing 50 mM EDTA. When HIV-1 NC was present in the reaction, the 2× formamide stop solution also contained 4 μg/mL DNA plasmid and 0.5% SDS. The samples were then denatured at 90 °C for 5 min and loaded on a 12% denaturing polyacrylamide gel. After electrophoresis, gels were dried under vacuum and exposed to an X-ray film (Kodak) or a PhosphorImager screen (Molecular Dynamics). Templated nucleotide incorporation reactions were performed in a similar manner but at 4 °C. For some studies, the typical RT binding buffer was replaced by a similar buffer but at pH 7.0 (RT binding buffer pH 7.0) or by one containing only 40 mM KCl (RT binding buffer 40 mM KCl).

Quantitation of Products on the Gels. The radioactivity in the gels was quantified by phosphorimaging; the data were

analyzed using ImageQuant software version 5.0. For each time point, the amount of unreacted substrate and the total amount of DNA in the lane (substrate and products) were quantified, the percentage of extended primer was calculated, and the results were plotted and fit as a function of time (variable *t*) using KaleidaGraph software.

Gel Retardation Assay. A blocked primer (blocked strand A) containing a dideoxycytidine at the 3′ end (BioSource International, Inc.) was 5′ end-labeled using [γ-^{32}P]ATP, and the excess [γ-^{32}P]ATP was removed by passing the labeling reaction through a G25 spin column (Roche Molecular Systems). The blocked strand A (containing up to 25% of ^{32}P-labeled molecules) was annealed to a template strand (strand B) added in 2-fold excess. The reaction conditions (DNA concentration, RT concentration, and buffer composition) of the gel retardation experiments were similar to those used for the kinetic experiments. The duplex (20 nM final) was incubated for 15 min with 200 nM HIV-1 RT in RT binding buffer 40 mM KCl containing 1 mM EDTA and 6 mM $MgCl_2$ in the presence of variable amounts of dATP. When specified, heparin (1 μg/mL final), 1 μM PBS duplex (5′ GTCCCTGTTCGGGCGCCA/5′ TGGCGCCCGAACAGGGAC), or 1 μM PBS duplex and 100 mM NaCl were added to the reaction as specified, and the mixture was incubated at 37 °C for 1 min or less as specified. Novex TBE sample buffer 6× (Novex) containing 45 mM Tris-HCl, 45 mM boric acid, 1 mM EDTA, 5.3% glycerol, 0.005% bromophenol blue, and 0.005% xylene cyanol was added, and the samples (4−6 μL) were immediately loaded on a 6% polyacrylamide (1/29 bisacrylamide/acrylamide)−TBE gel (1.5 or 3 mm thick) while the gel was running at 200 V. After 3 min, the voltage was decreased to 100 V. After electrophoresis, the gel was soaked in a solution containing 7% acetic acid and 2% glycerol for 5 min. The gel was dried under vacuum and exposed to a PhosphorImager screen or an X-ray film.

RESULTS

Slow Addition of Nontemplated dA to the 3′ End of a Blunt-Ended DNA/DNA Duplex. Although the mechanism of templated polymerization by HIV-1 RT is reasonably well characterized *(18−24)*, considerably less information is available about nontemplated nucleotide addition (*25−27*). To study nontemplated nucleotide addition, we prepared a blunt-ended DNA/DNA duplex substrate by annealing a labeled primer strand (strand A or a modified form of strand A) to an unlabeled template strand (strand B or a modified form of strand B) whose sequences derived from the HIV-1 genome (Table 1). The two strands formed a duplex that was blunt ended at the 3′ end of the primer strand.

We first used a complex formed by annealing strand A (primer) to strand B (template) (Table 1, Figure 1A). This blunt-ended duplex was 21 bp long and had a bulge at the 5′ end of the primer strand. Reactions were performed in RT binding buffer 40 mM KCl. After 20 nM duplex was preincubated at 37 °C for 5 min with 200 nM HIV-1 RT in the presence of 1 mM EDTA and 500 μM dATP, the reactions were started by the addition of 6 mM $MgCl_2$. Aliquots were quenched after various incubation times, and the products were analyzed on a 12% denaturing polyacrylamide gel (Figure 2A). Under these conditions, the duplex

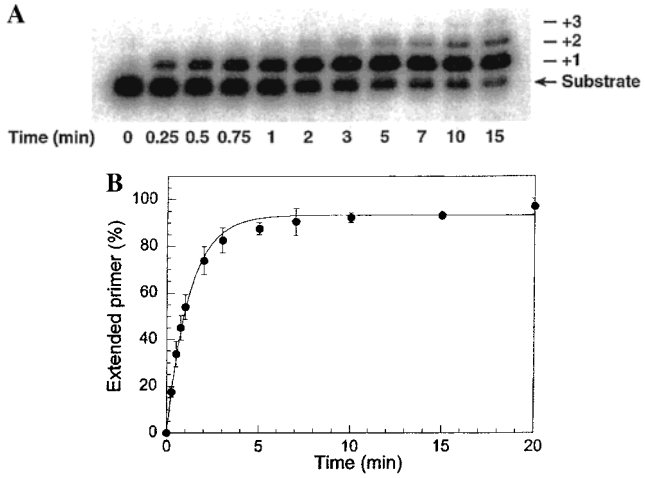

FIGURE 2: Nontemplated dATP addition to the 3′ end of the blunt-ended strand A/strand B duplex. (A) Autoradiogram representative of nontemplated addition of dATP to the 3′ end of the blunt-ended strand A/strand B duplex. 20 nM strand A/strand B duplex was preincubated at 37 °C for 5 min in RT binding buffer 40 mM KCl in the presence of 1 mM EDTA, 500 μM dATP, and 200 nM HIV-1 RT. At the indicated time points the reaction was started by the addition of 6 mM $MgCl_2$. Products were resolved on a 12% denaturing polyacrylamide gel. (B) For each time point, the percentage of primer extended by at least one base was calculated. The plot represents the average of three independent experiments. Data could be fit by a single exponential $[A_0(1 - \exp(-k_{obs}t))]$ with $A_0 = 89$ and $k_{obs} = 0.80$ min^{-1}.

was extended by up to three nucleotides. In the presence of higher concentrations of dATP or after longer incubation times, four to five dAs could be added to the 3′ end of the blunt-ended duplex (data not shown). The percentage of product (primer extended by at least one nucleotide), plotted as a function of the incubation time (Figure 2B), showed that the kinetics of nontemplated nucleotide addition was monophasic and the reaction went essentially to completion (the plateau was typically reached when ∼90% of the primer was extended). The time−course experiment could be fit by a single exponential $[A_0(1 - \exp(-k_{obs}t)]$ with $A_0 = 89$ and $k_{obs} = 0.80$ min^{-1} (Table 2). Similar experiments were performed with higher concentrations of substrate (20, 50, 100 nM) and RT (200, 500, 1000 nM, respectively). The values of the fit parameters were not affected by increasing the concentrations of substrate and RT, indicating that, in our initial experiment (20 nM substrate, 200 nM RT), the DNA was saturated and the apparent rate of the reaction (k_{obs}) was not affected by the K_d of RT for the duplex substrate.

If nucleotide addition is governed by rate-limiting Mg^{2+} binding, a lag in product formation would be predicted. However, we see no lag which shows that the binding of Mg^{2+} was in rapid equilibrium relative to the slow step of the reaction. When similar experiments were performed by preincubating all of the components except dATP for 5 min at 37 °C, and by starting the reactions by the addition of dATP, the kinetic parameters were not affected (data not shown). The absence of a lag under these conditions indicates that the binding of dATP was also in rapid equilibrium. Biphasic kinetics would place the rate-limiting step after the chemistry step; the absence of burst kinetics places the rate-limiting step at or prior to the chemistry step (dNTP-induced

Table 2: Rate of Nontemplated Nucleotide Addition with Blunt-Ended DNA/DNA Substrates[a]

substrate	dNTP	dNTP concn (μM)	k_{obs} (min^{-1})
strand A/strand B	dATP	500	$(8.0 \pm 1.5) \times 10^{-1}$
	dCTP	500	$(7.3 \pm 0.7) \times 10^{-3}$
	dGTP	500	$(1.1 \pm 0.2) \times 10^{-1}$
	dTTP	500	$(5.6 \pm 0.3) \times 10^{-3}$
	ddATP	500	$(3.7 \pm 1.0) \times 10^{-3}$
	ATP	500	0[d]
	dATP	10	$(3.4 \pm 0.9) \times 10^{-2}$
strand A/strand B + NC[b]	dATP	500	$(8.3 \pm 2.3) \times 10^{-1}$
strand A tail/strand B tail[c]	dATP	500	0[d]
	dCTP	500	$\sim 3 \times 10^{-4}$
	dGTP	500	$\sim 4 \times 10^{-4}$
	dTTP	500	$\sim 5 \times 10^{-4}$
strand A + dA/strand B	dATP	500	$(1.9 \pm 0.3) \times 10^{-2}$
	ATP	500	0[d]
strand A + dC/strand B	ATP	500	0[d]

[a] Reactions were performed in RT binding buffer 40 mM KCl as described in Materials and Methods. When reactions went to completion in a 1 h reaction, data were fit by a single exponential [$A_0(1 - \exp(-k_{obs}t))$]. For the reactions that did not go to completion, the linear part was fit by $A_0k_{obs}t$, and k_{obs} was calculated from the slope of the linear fit using $A_0 = 85$ (typical value of the amplitude of the exponential obtained with fast reactions). Each value is the average of at least four independent reactions. [b] The reactions were performed in RT binding buffer 40 mM KCl in the presence of a 2-fold excess of HIV-1 NC. [c] For these reactions, only the 1 h time point was made, and an estimate of k_{obs} was calculated by dividing the percentage of extended primer (0%, 1.6%, 2%, and 2.4% for dATP, dCTP, dGTP, and dTTP, respectively) by 60 (minutes) $\times$ 85 (typical value of the amplitude of the exponential for the reactions going to completion). [d] No extension of the primer was observed after 1 h.

conformational change or polymerization step) as reported for templated polymerization (*20*, *21*).

dATP Is Added to the Blunt-Ended Strand A/Strand B Duplex Faster Than the Other dNTPs. Similar reactions were performed with each of the three other dNTPs in place of dATP. The dGTP addition reaction went to completion during a 1 h reaction. As with dATP addition, the data could be fit by a single exponential (data not shown) with $k_{obs} = 0.11 \pm 0.02$ min^{-1} (Table 2). dCTP and dTTP additions were too slow to go to completion in 1 h. The data were fit using a linear regression with a slope equal to $85k_{obs}$ (85 corresponds to the average percentage of primer extension when the plateau was reached in reactions using dATP or dGTP). dCTP and dTTP were added at a much slower rate [$(7.3 \pm 0.7) \times 10^{-3}$ min^{-1} and $(5.6 \pm 0.3) \times 10^{-3}$ min^{-1}, respectively, Table 2]. With our experimental conditions and the specific blunt-ended DNA/DNA duplex that we used (strand A/strand B duplex), dATP was added $\sim$10 times faster than dGTP and approximately 100 times faster than dCTP and dTTP.

Is It Really Nontemplated Nucleotide Addition? We looked for possible secondary structures in strand A and found that it could fold back on itself and form a hairpin at its 3′ end (Figure 1B). With our buffer composition, the theoretical T_m (*17*) of this secondary structure was $\sim$55 °C; however, the T_m of the strand A/strand B duplex was above 80 °C. Theoretically, the formation of the strand A/strand B duplex would be favored relative to the formation of the hairpin at the 3′ end of strand A. We measured the quality of the annealing on a 6% nondenaturing polyacrylamide gel and found that, with our annealing conditions, more than 90% of strand A was part of a duplex (data not shown).

If a significant amount of a hairpin could be formed at the 3′ end of strand A, this end could be extended by templated nucleotide addition and dA would be the first nucleotide to be incorporated (Figure 1B). To determine whether the formation of such a secondary structure could contribute to the rapid incorporation of dATP (relative to the other dNTPs), we performed a reaction with only strand A in the annealing reaction and 500 μM dATP. dA addition was 50 times slower than when strand A and strand B were both present in the annealing step. Thus, the possible formation of a secondary structure did not contribute significantly to the faster incorporation of dA at the 3′ end of the blunt-ended duplex. This result was confirmed by using the blunt-ended strand A mutant/strand B mutant duplex (Table 2, Figure 1A). With this substrate, if strand A mutant folded back on itself, the first correct nucleotide to be incorporated would be dT and not dA (Figure 1B). However, the rate of dATP incorporation was not reduced by this mutation (data not shown). Thus, the faster dA incorporation cannot be explained by templated base addition due to hairpin formation at the 3′ end of strand A.

Another possibility would be that the first nucleotide was added by nontemplated nucleotide addition; then the overhang base could base pair with the 3′ end of a ssDNA molecule (excess of strand B or unannealed strand A molecules) and induce a one-base-pair strand transfer as we have described previously (*12*). With this mechanism, only the first nucleotide addition would be nontemplated. In such a case, strand transfer would occur only if the nontemplated nucleotide added to the 3′ end of the primer could form a base pair with the base at the 3′ end of a ssDNA molecule. The base at the 3′ end of both strand A and strand B is dC, which means that this mechanism would be more likely to occur in reactions in which dG is added to the end of the primer by nontemplated nucleotide addition. To determine whether this mechanism contributed to the addition of multiple nucleotides, we purified the duplex on a G50 spin column after annealing (to remove excess ssDNA) and performed a 1 h reaction in the presence of dGTP. The pattern of dGTP incorporation was not affected by the removal of the excess ssDNA (data not shown). These results indicate that the blunt-ended strand A/strand B duplex was formed during the annealing step and that the extension of strand A by several nucleotides was primarily due to nontemplated nucleotide addition to the 3′ end of the blunt-ended duplex.

The Affinity of the Incoming dNTP for a Complex Containing a Blunt-Ended Duplex Is Low. We studied the effects of the concentration(s) of dATP and dGTP on the rate of nontemplated nucleotide addition (Figure 3A); similar results were obtained with dATP and dGTP. For dNTP concentrations up to 1 mM, the rate of polymerization increased almost linearly with the concentration of dNTP. At higher concentrations, the experiments were less reproducible. The rate of polymerization tended to decrease, and the results were quite dependent on the source of the dNTP (Pharmacia, Gibco, Roche) (data not shown). The results obtained at high dNTP concentrations could be explained by the possible presence of small amounts of impurities in the dNTP solutions.

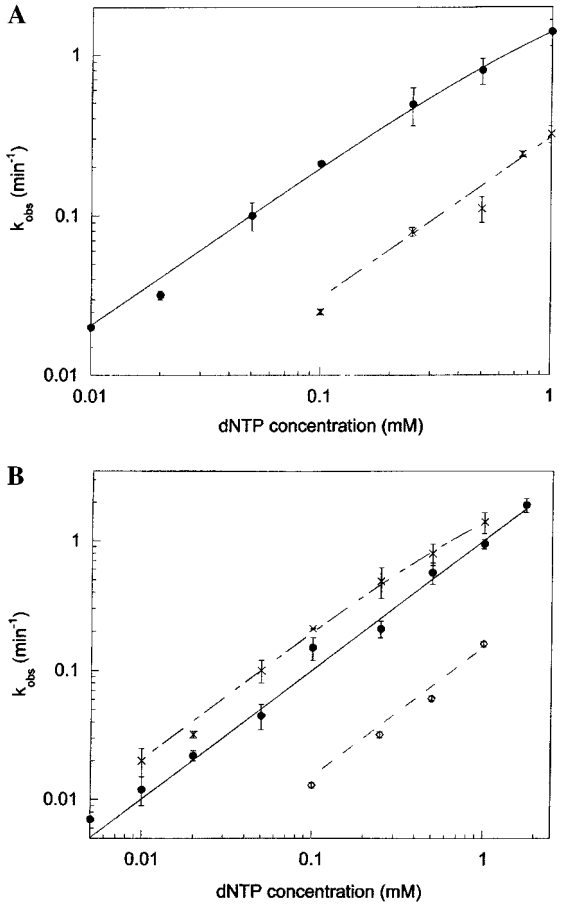

FIGURE 3: Effect of dNTP concentration, salt concentration, and pH of the reaction buffer on the rate of nontemplated nucleotide addition. (A) 20 nM blunt-ended strand A/strand B duplex was preincubated at 37 °C for 5 min in RT binding buffer 40 mM KCl in the presence of 1 mM EDTA, 200 nM HIV-1 RT, and a variable amount of dATP (●) or dGTP (×). The reactions were started by the addition of 6 mM $MgCl_2$. (B) 20 nM blunt-ended strand A/strand B duplex was preincubated at 37 °C for 5 min in RT binding buffer (●), RT binding buffer 40 mM KCl (×), or RT binding buffer pH 7.0 (◇) in the presence of 1 mM EDTA, 200 nM HIV-1 RT, and a variable amount of dATP. The reactions were started by the addition of 6 mM $MgCl_2$. Products were resolved on a 12% denaturing polyacrylamide gel. When reactions went to completion, data were fit with a single exponential. When the reactions did not go to completion, the linear part was fit by a linear regression, and k_{obs} was calculated from the slope. Each value of k_{obs} represents the average of at least three independent experiments.

The dependence of k_{obs} on the concentration of dNTP (Figure 3A) indicated that, even in the presence of 1 mM dATP or dGTP, saturation was not reached. If nucleotide incorporation is much slower than the dNTP binding step, $k_{obs} = k_{pol}[dNTP]/(K_d + [dNTP])$, where k_{obs} is the observed pre-steady-state rate, k_{pol} is the rate of polymerization at saturation, and K_d represents the equilibrium dissociation constant of the dNTP at the step just before the slowest step. The curves presented in Figure 3A did not allow us to make accurate hyperbolic fits. However, from these data, we could estimate that K_d values were at least 2 mM for both dATP and dGTP. For templated polymerization, the K_d for the incoming complementary nucleotide is typically ~5−10 μM (*19*, *20*, *22*, *23*, *28*, *29*). The low affinity for dNTPs in these nontemplated nucleotide addition reactions provides further evidence that the primer was not extended by a templated polymerization mechanism.

Table 3: Effects of Salt Concentration and pH on the Rate of Templated and Nontemplated Polymerization[a]

substrate	temp (°C)	pH	KCl concn (mM)	k_{obs} (min^{-1})
strand A/strand B	37	8.3	40	$(8.0 \pm 1.5) \times 10^{-1}$
	37	8.3	80	$(6.0 \pm 1.1) \times 10^{-1}$
	37	7.0	80	$(6.1 \pm 0.4) \times 10^{-2}$
strand A/strand B Pol	4	8.3	40	1.3 ± 0.2
	4	8.3	80	1.0 ± 0.2
	4	7.0	80	$(4.1 \pm 0.6) \times 10^{-1}$

[a] Reactions were performed in either RT binding buffer, RT binding buffer 40 mM, or RT binding buffer pH 7.0 in the presence of 500 μM dATP (strand A/strand B duplex) or 500 μM ddCTP (strand A/strand B Pol duplex) as described in Materials and Methods. When reactions went to completion in a 1 h reaction, data were fit by a single exponential $[A_0(1 - \exp(-k_{obs}t))]$. For the reactions that did not go to completion, the linear part of the curve was fit by the linear equation $A_0k_{obs}t$, and k_{obs} was calculated from the slope of the linear fit using $A_0 = 85$ (typical value of the amplitude of the exponential obtained with fast reactions). The nontemplated nucleotide addition (strand A/strand B duplex) reactions were run at 37 °C. The templated polymerization (strand A/strand B Pol duplex) reactions were run at 4 °C. Each value is the average of at least three independent experiments.

Effects of Salt Concentration and pH on the Rate of Nontemplated and Templated Polymerization. We studied the effects of salt concentration and pH on nontemplated nucleotide addition using the blunt-ended strand A/strand B duplex and 500 μM dATP in RT binding buffer (pH 8.3, 80 mM KCl), RT binding buffer 40 mM KCl (pH 8.3, 40 mM KCl), or RT binding buffer pH 7.0 (pH 7.0, 80 mM KCl). The results in Table 3 show that the rate of nontemplated nucleotide addition was not significantly affected by increasing the KCl concentration from 40 to 80 mM but k_{obs} decreased by a factor of 10 when the pH was decreased from 8.3 to 7.0 (at a KCl concentration of 80 mM). There are two distinct possibilities. The affinity for the dNTP could be affected (the reactions were not done at saturating concentrations of dNTP) or the rate of polymerization at saturation (k_{pol}) could be different. With the three buffers, the value of k_{obs} increased with the concentration of dATP, and saturation was never reached. In all cases, the estimated K_d was at least 2 mM dATP (Figure 3B).

Several previous studies have focused on the effects of pH and salt concentration on templated polymerization under multiple turnover (MTO) conditions (excess of nucleic acid substrate over RT) and, consequently, on the effects of these two parameters on the product release step which is rate limiting under MTO conditions (*30*−*32*). A DNA/DNA duplex formed by annealing strand A to strand B Pol (Table 1, Figure 1A) was used to study the effects of these parameters on polymerization under single turnover (STO) conditions (excess of RT over nucleic acid substrate) under conditions similar to those used to study nontemplated nucleotide addition. In this case, ddCTP was the first correct nucleotide to be incorporated. The K_d for a ddNTP complementary to the next base of a template is typically lower than 10 μM (*19*, *20*, *22*, *23*, *28*, *29*). We studied the effects of salt concentration and pH on templated nucleotide addition under STO conditions at saturating concentration of ddCTP (500 μM). In this case, the variations of the value of k_{obs} can be attributed to effects on k_{pol} (rate of polymerization at saturation) and not on the dissociation constant of the

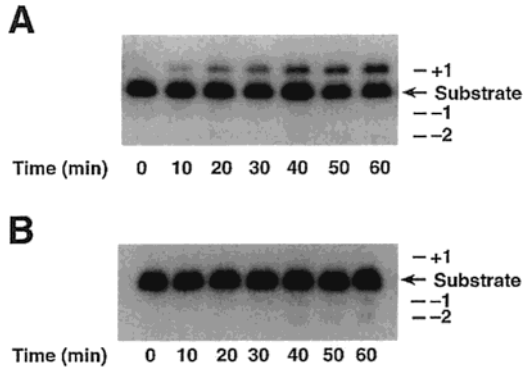

FIGURE 4: Nontemplated ddA and A additions to the 3′ end of the blunt-ended strand A/strand B duplex. 20 nM strand A/strand B duplex was preincubated at 37 °C for 5 min in RT binding buffer 40 mM KCl in the presence of 1 mM EDTA, 200 nM HIV-1 RT, and 500 μM ddATP (panel A) or 500 μM ATP (panel B). The reactions were started by the addition of 6 mM $MgCl_2$. Products were resolved on a 12% denaturing polyacrylamide gel.

nucleotide. To slow the rate of polymerization, the reactions were performed at 4 °C; as a consequence, the values of k_{obs} cannot be directly compared with those obtained for nontemplated nucleotide addition measured at 37 °C. With the strand A/strand B Pol duplex, decreasing the KCl concentration from 80 to 40 mM did not significantly affect the rate of templated polymerization, and decreasing the pH from 8.3 to 7.0 reduced k_{obs} only by a factor of 3 (Table 3).

Effect of the Type of Nucleoside Triphosphate on the Apparent Rate of Nontemplated Nucleotide Addition. For templated polymerization, replacement of a dNTP by a ddNTP does not significantly affect the K_d for the nucleoside triphosphate but reduces k_{pol} by at least a factor of 10 (*22*). The use of an NTP reduces the K_d by at least 50−100-fold whereas k_{pol} is reduced by 100−1000-fold (*20*). We performed experiments using the strand A/strand B duplex in RT binding buffer 40 mM KCl in the presence of 500 μM ddATP or ATP (Figure 4, Table 2). The addition of ddATP was more than 200 times slower than dATP addition. Under our experimental conditions, nontemplated ATP addition could not be observed during the time of the reaction (Figure 4). In this case, while the primer was not extended, i.e., there was no nontemplated nucleotide addition, excision products were produced due to pyrophosphorolysis (*23*, *33*−*35*).

High Concentrations of ATP Can Significantly Reduce Nontemplated Nucleotide Addition. In vivo, dNTP concentrations are typically ∼5−10 μM, and the ATP concentration is around 3 mM. We found that the rate of nontemplated dATP addition was dependent on the concentration of dATP and that ATP was a poor substrate for nontemplated polymerization. Moreover, it is known that, with a nucleic acid duplex with a template overhang, ATP can participate in pyrophosphorolysis reactions (*23*, *33*−*35*) and/or bind weakly to the polymerase active site (*20*, *36*). We measured the effect of ATP on the nontemplated addition of dATP using in vivo concentrations of dATP (10 μM). In the absence of ATP, ∼60% of the primer was extended after 1 h (Figure 5A). In the presence of 3 mM ATP, very little nontemplated nucleotide addition was observed, and shorter products were formed due to pyrophosphorolysis (Figure 5B). When both 10 μM dATP and 3 mM ATP were present, there was both extension of the primer by nontemplated nucleotide addition and excision of the primer by pyrophosphorolysis (Figure 5C); furthermore, the amount of excision products (products shorter than the primer before the reaction) was reduced relative to the products seen in reactions performed in the presence of only 3 mM ATP. This difference is probably the result of extension of some of the excision products by templated nucleotide addition due to the presence of dATP; there was less extended primer than when only dATP was present. Quantitation of the amount of extended primer in each reaction (Figure 5D) showed that the rate of nontemplated nucleotide addition when both dATP and ATP were present was approximately half of the rate when only dATP was present. There are two possible explanations for this result. Primers extended by nontemplated nucleotides could be a substrate for pyrophosphorolysis, and the slower apparent rate of nontemplated nucleotide addition could reflect a competition between nontemplated polymerization and pyrophosphorolysis. Alternatively, at high concentrations, ATP could compete for binding to the dNTP-binding pocket; only complexes with dATP in the dNTP-binding pocket could carry out nontemplated nucleotide addition.

Duplexes with a Primer Extended by One Nontemplated Nucleotide Are Poor Substrates for Nontemplated Nucleotide Addition and Pyrophosphorolysis. The DNA/DNA duplex containing strand A + dA and strand B (Table 1, Figure 1A) represented the product formed by addition of one nontemplated dA to the 3′ end of the blunt-ended strand A/strand B duplex. In the presence of 500 μM dATP, nontemplated nucleotide addition occurred (Figure 6A) but was much slower than with the strand A/strand B duplex ($k_{obs} = 1.9 \times 10^{-2}$ min^{-1} and $k_{obs} = 0.8$ min^{-1}, respectively; Table 2). Similar experiments were performed with twice as much of the strand A + dA/strand B duplex and RT. The values of the fit parameters were not affected, indicating that the slower k_{obs} was not due to a poor affinity of RT for this substrate.

Similar experiments were performed in the presence of 3 mM ATP (Figure 6B). As for the strand A/strand B duplex, nontemplated addition of ATP was not observed. There was no measurable pyrophosphorolysis. When experiments were performed with a duplex formed by annealing strand A + dC to strand B (model of the product of nontemplated dC addition to the blunt-ended strand A/strand B duplex; Table 1, Figure 1A), similar results were obtained with ATP (Table 2). These results showed that duplexes with a one-nucleotide overhang on the primer were not good substrates for pyrophosphorolysis. Because there was no competition between nontemplated nucleotide addition to a blunt-ended duplex and removal of the nontemplated nucleotide by pyrophosphorolysis, the reduction in the rate of nontemplated dA addition to the blunt-ended strand A/strand B duplex seen in the presence of a large concentration of ATP was likely due to competition between the ATP and dATP for the dNTP-binding pocket.

Nontemplated Nucleotide Addition with the Strand A Tail/Strand B Tail Duplex. Similar experiments were performed with a blunt-ended duplex formed by annealing strand A tail to strand B tail (Table 1). In this case, the 3′ end of the primer strand was formed by five A's double-stranded with five T's (Figure 1A). Addition of a dNTP was quite slow (less than 3% of the primer was extended after 1 h in the fastest reaction; Figure 7). No nucleotide addition was seen with dATP. Of the four dNTPs, dTTP addition was the fastest

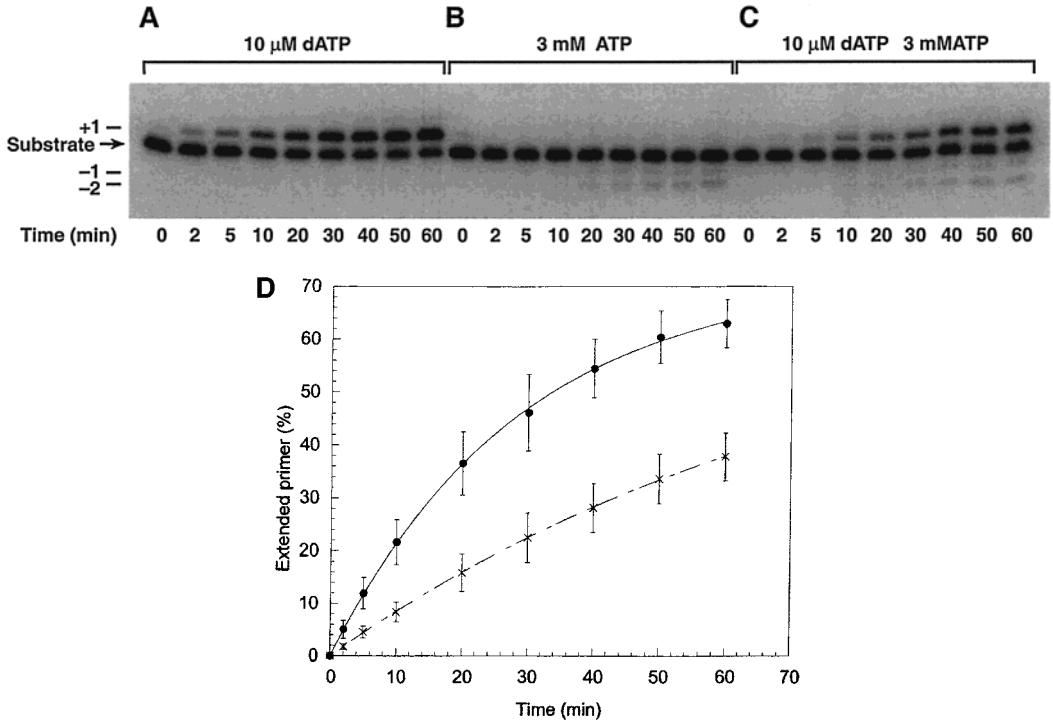

FIGURE 5: High concentrations of ATP reduce nontemplated addition of dATP. 20 nM strand A/strand B duplex was preincubated at 37 °C for 5 min in RT binding buffer 40 mM KCl in the presence of 1 mM EDTA, 200 nM HIV-1 RT, and either 10 μM dATP (panel A), 3 mM ATP (panel B), or 10 μM dATP and 3 mM ATP (panel C). The reactions were started by the addition of 6 mM $MgCl_2$. Products were resolved on a 12% denaturing polyacrylamide gel. (D) Extension of the blunt-ended strand A/strand B duplex in the presence of 10 μM dATP (●) or 10 μM dATP and 3 mM ATP (×) as a function of the incubation time. The conditions of the reaction are similar to those described previously. The curves are the average of seven independent experiments.

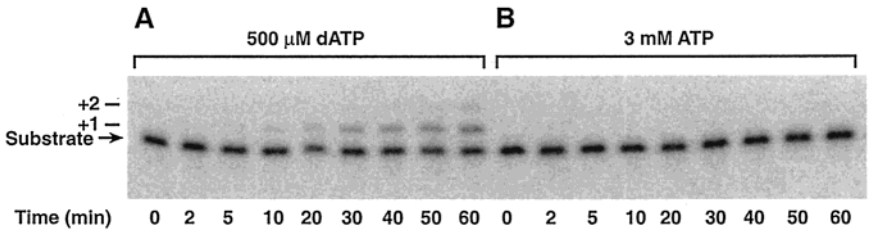

FIGURE 6: The strand A + dA/strand B duplex is a poor substrate for nontemplated nucleotide addition and pyrophosphorolysis. 20 nM strand A + dA/strand B duplex was preincubated at 37 °C for 5 min in RT binding buffer 40 mM KCl in the presence of 1 mM EDTA, 200 nM HIV-1 RT, and 500 μM dATP (panel A) or 3 mM ATP (panel B). The reactions were initiated by the addition of 6 mM $MgCl_2$. Products were resolved on a 12% denaturing polyacrylamide gel.

reaction. The preference for the addition of dATP over the other deoxynucleotides observed with the blunt-ended strand A/strand B duplex was not seen with the blunt-ended strand A tail/strand B tail duplex. Thus, both the rate and the specificity of nontemplated nucleotide addition were strongly affected by the sequence at the 3′ end of the primer strand.

Nontemplated dATP Addition to a Blunt-Ended RNA/DNA Duplex. Nontemplated nucleotide addition experiments were performed with a duplex formed by a DNA primer and an RNA template (strand A/strand B RNA duplex; Table 1, Figure 1A). These experiments were performed in RT binding buffer 40 mM KCl in the presence of 500 μM dATP (Figure 8). The data cannot be fit with a single exponential but do fit a double-exponential equation $[A_1(1 - \exp(-k_1 t)) + A_2(1 - \exp(-k_2 t)]$. The amplitude of the first exponential was small (about 10% of the extended primer). Consequently, the error in estimating the rate of the first exponential (k_1) was relatively large (2.0 ± 0.6 min^{-1}) (Table 4); k_2 was much slower [$(7.0 \pm 1.4) \times 10^{-2}$ min^{-1}]. One possible explanation for this biphasic behavior would be that strand A was only partially hybridized to strand B RNA, and the rapid first phase would correspond to the nontemplated addition of dA

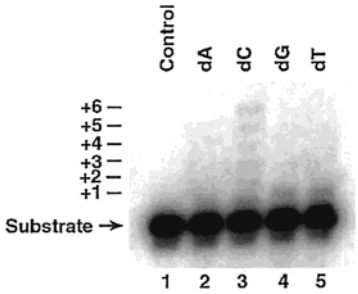

FIGURE 7: Nontemplated nucleotide addition to the 3′ end of the blunt-ended strand A tail/strand B tail duplex. 20 nM strand A tail/strand B tail duplex was preincubated at 37 °C for 5 min in RT binding buffer 40 mM KCl in the presence of 1 mM EDTA, 200 nM HIV-1 RT, and no dNTP (lane 1), 500 μM dATP (lane 2), dCTP (lane 3), dGTP (lane 4), or dTTP (lane 5). The reactions were initiated by the addition of 6 mM $MgCl_2$. After 1 h, the reactions were quenched, and products were resolved on a 12% denaturing polyacrylamide gel.

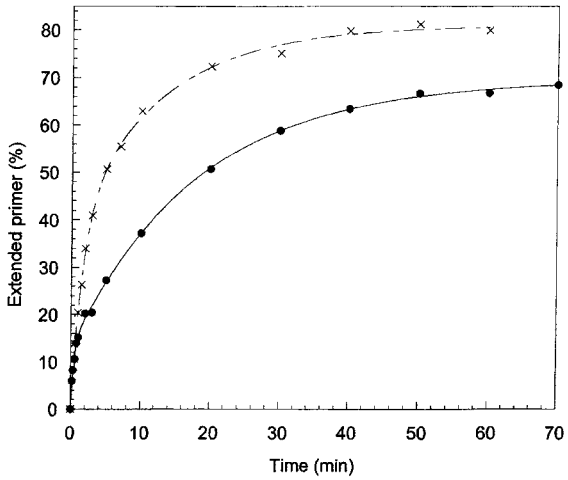

FIGURE 8: Nontemplated dA addition to blunt-ended RNA/DNA duplexes. 20 nM blunt-ended strand A/strand B RNA (●) or strand A 41-mer/HIV-1 R RNA (×) duplex was preincubated at 37 °C for 5 min in RT binding buffer 40 mM KCl in the presence of 1 mM EDTA, 200 nM HIV-1 RT, and 500 μM dATP. The reactions were initiated by the addition of 6 mM $MgCl_2$. Products were resolved on a 12% denaturing polyacrylamide gel. Data were fit by a double-exponential equation $[A_1(1 - \exp(-k_1t)) + A_2(1 - \exp(-k_2t))]$.

Table 4: Rate of Nontemplated Nucleotide Addition with Blunt-Ended DNA/DNA and DNA/RNA Substrates[a]

substrate	A_1 (%)	k_1 (min^{-1})	k_2 (min^{-1})
strand A/ strand B	89 ± 2	(8.0 ± 1.5) × 10^{-1}	
strand A/ strand B RNA	10 ± 4	2.0 ± 0.6	(7.0 ± 1.4) × 10^{-2}
strand A short/ strand B RNA	15 ± 4	1.1 ± 0.3	(6.0 ± 2.1) × 10^{-2}
strand A long/ strand B long	85 ± 3	1.1 ± 0.1	
strand A long/ strand B long RNA	36 ± 3	(9.5 ± 2.0) × 10^{-1}	(4.3 ± 1.9) × 10^{-2}
strand A 41-mer/ HIV-1 R RNA	42 ± 10	(7.2 ± 1.4) × 10^{-1}	(7.8 ± 2.1) × 10^{-2}

[a] Reactions were performed in RT binding buffer 40 mM KCl as described in Materials and Methods. Data were fit using a double-exponential equation $[A_1(1 - \exp(-k_1t)) + A_2(1 - \exp(-k_2t))]$ for DNA/RNA duplex substrates and using a single-exponential equation $[A_1(1 - \exp(-k_1t))]$ for DNA/DNA duplex substrates. Each value is the average of at least four independent experiments.

to the blunt-ended duplex and the amplitude of the first exponential would correspond to the portion of strand A that was double stranded at the beginning of the reaction. The slower second phase would then reflect the slow annealing of the remaining strand A. When we performed these experiments with a larger excess of strand B RNA over strand A (up to a 10-fold excess), the amplitude of the first exponential did not increase (data not shown), indicating that the biphasic nature of the reaction was not due to poor annealing of the two strands.

Experiments performed with a duplex formed by strand A short annealed to strand B RNA (Table 1, Figure 1A) gave similar results, showing that the removal of the bulge at the 5′ end of the primer strand did not significantly affect the reaction (Table 4). From experiments performed with a duplex formed by strand A 41-mer annealed to HIV-1 R RNA (Table 1), the data could be fit by a double-exponential (Figure 8) equation, but the amplitude of the first exponential was much larger (42 ± 10%) while the rates of the two exponentials were not affected (0.7 ± 0.1 min^{-1} and 0.08 ± 0.02 min^{-1}, respectively). Similar results were obtained when the strand A long/strand B long RNA duplex was used (Tables 1 and 4, Figure 1A). With the strand A long/strand B long (DNA/DNA) duplex, the data could be fit by a single exponential with a rate of 1.1 ± 0.1 min^{-1}. Thus, with the DNA/DNA duplex, the kinetics were always monophasic, and the rate of nontemplated nucleotide addition was not affected by the length of the DNA template strand. In the case of the RNA/DNA duplex, the kinetics were biphasic, and the amplitude of the first phase increased with the length of the RNA template, but the rates were not significantly affected.

HIV-1 NC Does Not Reduce Nontemplated Nucleotide Addition. Experiments using the strand A/strand B blunt-ended duplex were performed in the presence of 500 μM dATP and a 2-fold excess of HIV-1 NC. The excess of HIV-1 NC was calculated assuming that each NC molecule covers seven bases (*37*). Nontemplated dA addition was not affected by the presence of HIV-1 NC (Table 2), even when the reactions were performed with an 8-fold excess of HIV-1 NC (data not shown).

RT Did Not Form a Stable Ternary Complex with Blunt-Ended DNA/DNA Duplexes. For duplexes with a template overhang, the RT/nucleic acid binary complex is considerably weaker than the ternary complex (*19*, *38*); the ternary complex is also weaker before the conformational change than after. The conformational change can be studied under conditions where the chain extension is blocked. RT complexed with a nucleic acid substrate in which the primer lacks a 3′-hydroxyl group can bind the next complementary dNTP, thus forming a dead-end complex that can be identified by its slow rate of dissociation (*19*, *38*). The stable ternary complex can be detected using a gel retardation assay (*13*, *14*). The structure of the nucleic acid/RT/dNTP complex after the conformational change has been solved (*39*).

We used gel retardation assays to study the stability of the complex formed by RT and a blunt-ended DNA/DNA duplex. Strand A was blocked by replacing the dC at the 3′ end of the primer with ddC (blocked strand A; Table 1). The experimental conditions (salt concentration, pH, and concentrations of the duplex substrate and RT) were similar to those used in the kinetic studies. With the blocked strand A/strand B Pol duplex (Figure 1A) that had a six-nucleotide template overhang, most of the duplex substrate was bound to RT even in the absence of dCTP, which was complementary to the first base of the template overhang (Figure 9A, lane 1). The amount of the RT-DNA/DNA duplex complex was not increased by large concentrations of dCTP (Figure 9A, lane 2). A 1 min chase with an unlabeled DNA duplex (lanes 11−18) was not able to separate the binary complex from the ternary complex, and no clear differences in the amount of shifted duplex could be seen as a function of the dCTP concentration. Similar results were obtained with a 1 min heparin chase (lanes 3−10). When the chase was performed by adding unlabeled DNA duplex and by increasing the salt concentration by 100 mM, the amount of shifted complex increased with increasing concentrations of dCTP (lanes 19−26). Similar experiments were performed with the blunt-ended blocked strand A/strand B duplex (Figure 9B). In the absence of a chase (lanes 1 and 2), most of the duplex was shifted, and there were no differences in the amount of

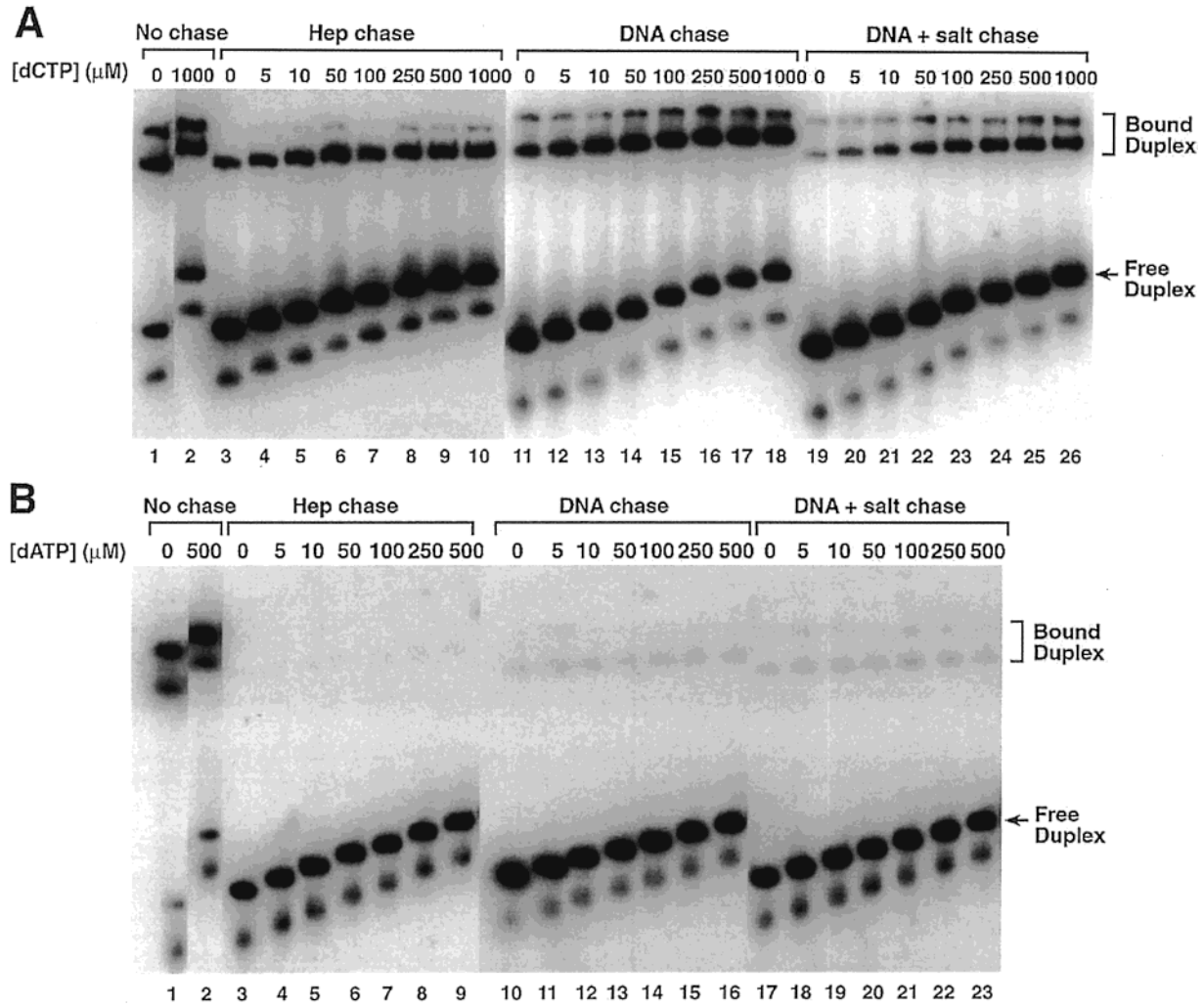

FIGURE 9: Formation of the ternary complex with the blocked strand A/strand B Pol and the blocked strand A/strand B duplexes. (A) 20 nM blocked strand A/strand B Pol was incubated in RT binding buffer 40 mM KCl in the presence of 1 mM EDTA, 6 mM $MgCl_2$, and variable amounts of dCTP for 15 min. The samples were immediately loaded on a 6% nondenaturing polyacrylamide gel (lanes 1 and 2) or chased for 1 min before being loaded by the addition of heparin (lanes 3−10), unlabeled DNA duplex (lanes 11−18), or unlabeled DNA duplex and 100 mM NaCl (lanes 19−26). (B) 20 nM blocked strand A/strand B was incubated in RT binding buffer 40 mM KCl in the presence of 1 mM EDTA, 6 mM $MgCl_2$, and variable amounts of dATP for 15 min. The samples were directly loaded on a 6% nondenaturing polyacrylamide gel (lanes 1 and 2) or chased for 1 min before being loaded by addition of heparin (lanes 3−9), unlabeled DNA duplex (lanes 10−16), or unlabeled DNA duplex and 100 mM NaCl (lanes 17−23). To avoid problems with disassociation of the complex, the samples were loaded onto the gel at different times with the gel running (see Materials and Methods). As a consequence, the samples loaded first migrated the farthest.

complex as a function of the dATP concentration (0−500 μM). However, if the reactions were subjected to a 1 min chase with heparin (lanes 3−9), unlabeled DNA duplex (lanes 10−16), or unlabeled DNA duplex and 100 mM NaCl (lanes 17−23), the band corresponding to the complex formed by HIV-1 RT and the DNA substrate disappeared, and no differences could be seen as a function of the dATP concentration. If the unlabeled DNA duplex was added and the sample was immediately loaded on the gel (the chase time could be estimated at about 5−10 s), more shifted substrate could be seen, but again, the dATP concentration made no difference (data not shown). Experiments were performed with even larger dATP concentrations (1−20 mM), and again, no shifted band remained after the chase (data not shown). It was easier to chase the binary complex when a blunt-ended duplex was used than when there was a template overhang. Although RT was able to bind blunt-ended duplexes, the stability was much lower than if the duplex had a template overhang. The fact that we could find chase conditions which differentiated the stable ternary complex formed after the conformational change from the binary complex with a DNA/DNA duplex that had a template overhang but not with a blunt-ended DNA/DNA duplex indicates either that the stability of the complex with a blunt-ended duplex after the conformational change is considerably reduced or that the conformational change does not occur.

DISCUSSION

We studied nontemplated nucleotide addition by HIV-1 RT under STO conditions (large excess of HIV-1 RT relative to the nucleic acid substrate). With the blunt-ended DNA/DNA duplex formed by strand A and strand B (primer and template strands, respectively; Table 1, Figure 1A), the addition of a nontemplated nucleotide was monophasic. This behavior indicates that the slow step occurred at or before the chemistry step. The K_d for dNTP was at least 2 mM. dNTPs were added ~200 times faster than ddNTPs; insertion of NTPs was not observed at concentrations up to 500 μM.

This preference for dNTPs is similar to what was observed for templated polymerization (*20*, *22*). At 500 μM, dATP was added ~10 times faster than dGTP and 100 times faster than dCTP and dTTP. This specificity was completely lost with the blunt-ended strand A tail/strand B tail duplex. Moreover, with this duplex, the reaction was much slower. Previously, we found that, with a blunt-ended duplex whose sequence was identical to the 3′ end of HIV-2 −R ssDNA, dATP and dCTP were added the most efficiently by HIV-1 RT (*12*). Previous studies of nontemplated nucleotide addition by diverse DNA polymerases showed that the efficiency and specificity of nontemplated nucleotide addition are highly dependent on the sequence of the 3′ end of the primer (*40*, *41*); however, Patel et al. (*25*) proposed that nontemplated nucleotide addition by HIV-1 RT is highly specific for the addition of deoxypurine nucleotide (dA better than dG). Although nontemplated nucleotide addition may be more efficient with deoxypurines (more specifically with dATP), the efficiency and specificity of nontemplated nucleotide addition by HIV-1 RT are clearly dependent on the sequence at the 3′ end of the blunt-ended template-primer duplex.

Under our experimental conditions, the K_d for dATP was at least 2 mM. With a duplex containing a template overhang, the K_d for the dNTP complementary to the first base of the template overhang is typically ~5−10 μM (*19*, *20*, *22*, *23*, *28*, *29*). When the incoming dNTP is not complementary to the first base of the template overhang (formation of a mismatch), the K_d is also in the millimolar range (*19*, *20*), as it is for nontemplated nucleotide addition. It has been proposed that the formation of hydrogen bonds between the incoming dNTP and the first base of the template overhang is not essential for high efficiency and fidelity of DNA synthesis and that the shape of the base plays an important role (*42*). Our results indicate that the absence of a template overhang significantly reduces the affinity for the incoming dNTP and, consequently, that formation of hydrogen bonds between the incoming dNTP and the template base contributes significantly to dNTP binding. In the absence of a template overhang, the efficiency of dNTP binding can be affected by the structure and geometry of the base (how well it fits into the active site of RT) or by stacking interactions between the incoming dNTP and the last base at the 3′ end of the primer. It is possible that deoxypurines fit better into the active site of RT, but, at least with certain specific sequences at the 3′ end of the primer strand, stacking interactions may also contribute to a preference for certain incoming dNTPs.

Although the salt concentration had only modest effects on the observed rate of nontemplated nucleotide addition, the rate was reduced by a factor of ~10 when the pH of the reaction was reduced from 8.3 to 7.0. A similar change in the pH had a more limited effect on templated polymerization performed at saturating dNTP concentration (reduction by a factor of ~2). These results are in agreement with the observation that the fidelity of HIV-1 RT in vitro was increased at pH 6.0 relative to pH 8.6 (*43*).

Because the affinity for dNTPs is very low with a blunt-ended substrate, nontemplated nucleotide addition is much slower than templated nucleotide addition at in vivo dNTP concentrations (~5−10 μM). Moreover, in the presence of 3 mM ATP (a typical in vivo ATP concentration), the rate of the reaction is even slower. We found that duplexes with a dA or a dC overhang on the primer strand are not substrates for the excision reaction. The reduction in the rate of nontemplated nucleotide addition cannot be explained by excision of the nontemplated nucleotide by pyrophosphorolysis reaction as has been suggested (*35*). Ribonucleotides can be incorporated during templated polymerization, but the dissociation constant for an NTP is 50−500 times higher than for a dNTP (*20*). At in vivo concentrations, NTPs cannot compete with dNTPs for binding to the polymerase active site during templated polymerization. However, in the case of a blunt-ended duplex, the K_d for dATP is in the millimolar range. We propose that the reduction of nontemplated nucleotide addition in the presence of in vivo concentrations of ATP and dATP (3 mM and 10 μM, respectively) is primarily due to competition between dATP and ATP for binding to the active site of RT. Nontemplated nucleotide addition is not affected by NC protein. For both mismatch formation and nontemplated nucleotide addition, the K_d for the incoming dNTP is in the millimolar range whereas the K_d for the dNTP complementary to the first base of the template overhang is in the micromolar range. Using high concentrations of dNTPs in the absence of ATP will increase the binding and incorporation of noncomplementary dNTPs to templated primers and dNTPs to blunt-ended duplexes, both of which will increase the error rate of RT. Thus, in vitro studies of RT fidelity performed at dNTP concentrations much higher than the concentrations present in vivo and in the absence of millimolar concentrations of ATP may overestimate the number of errors made during reverse transcription.

When a blunt-ended duplex is formed due to a break in the RNA template or because RT reaches the capped 5′ end of the RNA, there is competition between nontemplated nucleotide addition and specific strand transfer to the other RNA copy. We measured the rate of annealing of strand A to strand B Pol (duplex with 21 base pairs; Figure 1A) and found that, in the absence of NC, the second-order rate constant of the annealing of the two strands was ~6.7×10^5 min^{-1} M^{-1}. In the presence of a 2-fold excess of NC, the rate was increased by at least 3-fold (~2.7×10^6 min^{-1} M^{-1}). Moreover, the rate of the strand transfer increased with the number of base pairs that can be formed between the donor strand and the acceptor strand (data not shown). Thus, at in vivo dNTP concentrations, specific strand transfer is much faster than nontemplated nucleotide addition, and this difference increases in the presence of NC. Moreover, when efficient nontemplated nucleotide addition at the 3′ end of the DNA strand was observed before strand transfer, after strand transfer the frequency of errors at the site of strand transfer in DNA was much lower after strand transfer (*26*). Similar observations were made in in vivo studies with murine leukemia virus (MLV) and Ty1 (*8*, *44*). Moreover, there were no mutations arising from the addition of more than one nontemplated nucleotide, indicating that the extended products are poor substrates for strand transfer or, more likely, for extension after strand transfer *(26, 27)*. Thus, the frequency of mutations due to nontemplated nucleotide addition before strand transfer seems to be reduced by the low efficiency of nontemplated nucleotide addition under in vivo conditions, because specific strand transfer is much faster than nontemplated nucleotide addition, and by a selection against the use of primers that have been extended

by a nontemplated nucleotide either at the step of the strand transfer or just after (inefficient extension of a primer terminated by a mismatch).

The kinetics of nontemplated nucleotide addition with RNA/DNA duplexes were biphasic. This type of behavior was observed previously (*20*, *45*−*48*) and has generally been attributed to the existence of two different states of the substrate/RT complex. The first rapid phase corresponds to the reaction of the more active complex whereas the second slower phase corresponds to the reaction of the second slower complex or to the rate of conversion of a nonproductive complex to a productive complex. When we increased the length of the duplex, the amplitude of the first phase increased whereas the other kinetic parameters were not affected. Such biphasic behavior was not observed with the DNA/DNA duplexes used in this study. Crystallographic studies of a DNA/DNA-RT complex (*39*, *49*) and a DNA/RNA-RT complex (*50*) showed that RT makes more contacts with an RNA template than with a DNA template. With an RNA/DNA substrate, the last base in contact with RT is ∼20 bp from the 3′ end of the primer (*50*). The strand A/strand B RNA duplex used in this study contained only 21 bp. It is possible that the small number of base pairs in this duplex, together with the increased contacts between RT and the RNA template (relative to a DNA template), is responsible for the biphasic kinetics observed with DNA/RNA substrates. This could explain why the amplitude of the first phase increased with longer duplexes (a longer duplex has more contacts with RT). It is possible that the short size of the primer strand affects the number of contacts between RT and the substrate at the RNase H active site or affects the positioning of RT on the substrate. It is also possible, because an RNA/DNA duplex is a substrate for the RNase H activity of HIV-1 RT, that cleavage of the RNA template affects the rate of addition of nontemplated nucleotides.

We showed by gel retardation assay that, under our experimental conditions (20 nM duplex, 200 nM RT), the substrate was bound to RT (duplex shifted by RT in the absence of a chase), indicating a K_d (RT/substrate) lower than 20 nM. The K_d for a nucleic acid with a template overhang is ∼5 nM (*19*, *22*). With a blunt-ended duplex, as soon as a chase step was added (either an unlabeled DNA duplex or heparin), the binary duplex was lost; in contrast, with a duplex with a template overhang, a similar chase did not significantly reduce the amount of the binary complex. Thus, the absence of template overhang significantly increased the dissociation rate of the binary complex. Moreover, with a blunt-ended substrate we were not able to observe the ternary complex by using a gel retardation assay whereas, under similar conditions, the ternary complex was observed with a duplex with a template overhang. This confirms observations from Tong et al. (*14*) that, if the template strand is only a few bases longer than the primer, small amounts of a ternary complex were observed by gel retardation assay, and this amount decreases as the size of the template overhang decreases. Crystallographic studies of DNA/DNA duplex-RT and DNA/RNA duplex-RT complexes showed that RT makes contact with the template overhang (*39*, *49*, *50*). The increase of the dissociation rates of the binary and ternary complexes indicates that contacts between RT and the template overhang are important for stabilization of the binary and ternary complexes.

ACKNOWLEDGMENT

We are grateful to Robert Gorelick, Louis Henderson, and Larry Arthur for the gift of HIV-1 NC. We are also grateful to Anne Arthur for expert editorial assistance. We thank Pat Clark and Peter Frank for preparing purified HIV-1 RT and Hilda Marusiodis for help in preparing the manuscript.

REFERENCES

1. Goff, S. P. (1990) *J. Acquired Immune Defic. Syndr. 3*, 817−831.
2. Whitcomb, J. M., and Hughes, S. H. (1992) *Annu. Rev. Cell Biol. 8*, 275−306.
3. Coffin, J. M., Hughes, S. H., and Varmus, H. E. (1997) *Retroviruses*, Cold Spring Harbor Laboratory Press, Plainview, NY.
4. Hughes, S. H., Hostomsky, Z., Le Grice, S. F., Lentz, K., and Arnold, E. (1996) *J. Virol. 70*, 2679−2683.
5. Palaniappan, C., Fuentes, G. M., Rodriguez-Rodriguez, L., Fay, P. J., and Bambara, R. A. (1996) *J. Biol. Chem. 271*, 2063−2070.
6. Schatz, O., Mous, J., and Le Grice, S. F. (1990) *EMBO J. 9*, 1171−1176.
7. Coffin, J. M. (1979) *J. Gen. Virol. 42*, 1−26.
8. Kulpa, D., Topping, R., and Telesnitsky, A. (1997) *EMBO J. 16*, 856−865.
9. Panganiban, A. T., and Fiore, D. (1988) *Science 241*, 1064−1069.
10. Driscoll, M. D., and Hughes, S. H. (2000) *J. Virol. 74*, 8785−8792.
11. Golinelli, M.-P., and Hughes, S. H. (2001) *Virology 285*, 278−290.
12. Golinelli, M.-P., and Hughes, S. H. (2002) *Virology 294*, 122−134.
13. Gao, H. Q., Boyer, P. L., Sarafianos, S. G., Arnold, E., and Hughes, S. H. (2000) *J. Mol. Biol. 300*, 403−418.
14. Tong, W., Lu, C. D., Sharma, S. K., Matsuura, S., So, A. G., and Scott, W. A. (1997) *Biochemistry 36*, 5749−5757.
15. Boyer, P. L., Tantillo, C., Jacobo-Molina, A., Nanni, R. G., Ding, J., Arnold, E., and Hughes, S. H. (1994) *Proc. Natl. Acad. Sci. U.S.A. 91*, 4882−4886.
16. Adachi, A., Gendelman, H. E., Koenig, S., Folks, T., Willey, R., Rabson, A., and Martin, M. A. (1986) *J. Virol. 59*, 284−291.
17. SantaLucia, J., Jr. (1998) *Proc. Natl. Acad. Sci. U.S.A. 95*, 1460−1465.
18. Majumdar, C., Abbotts, J., Broder, S., and Wilson, S. H. (1988) *J. Biol. Chem. 263*, 15657−15665.
19. Kati, W. M., Johnson, K. A., Jerva, L. F., and Anderson, K. S. (1992) *J. Biol. Chem. 267*, 25988−25997.
20. Zinnen, S., Hsieh, J. C., and Modrich, P. (1994) *J. Biol. Chem. 269*, 24195−24202.
21. Hsieh, J. C., Zinnen, S., and Modrich, P. (1993) *J. Biol. Chem. 268*, 24607−24613.
22. Reardon, J. E. (1992) *Biochemistry 31*, 4473−4479.
23. Reardon, J. E. (1993) *J. Biol. Chem. 268*, 8743−8751.
24. Wöhrl, B. M., Krebs, R., Goody, R. S., and Restle, T. (1999) *J. Mol. Biol. 292*, 333−344.
25. Patel, P. H., and Preston, B. D. (1994) *Proc. Natl. Acad. Sci. U.S.A. 91*, 549−553.
26. Peliska, J. A., and Benkovic, S. J. (1994) *Biochemistry 33*, 3890−3895.
27. Peliska, J. A., and Benkovic, S. J. (1992) *Science 258*, 1112−1118.
28. Spence, R. A., Anderson, K. S., and Johnson, K. A. (1996) *Biochemistry 35*, 1054−1063.
29. Spence, R. A., Kati, W. M., Anderson, K. S., and Johnson, K. A. (1995) *Science 267*, 988−993.
30. Hoffman, A. D., Banapour, B., and Levy, J. A. (1985) *Virology 147*, 326−335.

31. St. Clair, M. H., Richards, C. A., Spector, T., Weinhold, K. J., Miller, W. H., Langlois, A. J., and Furman, P. A. (1987) *Antimicrob. Agents Chemother. 31*, 1972−1977.
32. Kruhoffer, M., Urbanke, C., and Grosse, F. (1993) *Nucleic Acids Res. 21*, 3943−3949.
33. Meyer, P. R., Matsuura, S. E., So, A. G., and Scott, W. A. (1998) *Proc. Natl. Acad. Sci. U.S.A. 95*, 13471−13476.
34. Meyer, P. R., Matsuura, S. E., Schinazi, R. F., So, A. G., and Scott, W. A. (2000) *Antimicrob. Agents Chemother. 44*, 3465−3472.
35. Boyer, P. L., Sarafianos, S. G., Arnold, E., and Hughes, S. H. (2001) *J. Virol. 75*, 4832−4842.
36. Boyer, P. L., Sarafianos, S. G., Arnold, E., and Hughes, S. H. (2000) *Proc. Natl. Acad. Sci. U.S.A. 97*, 3056−3061.
37. You, J. C., and McHenry, C. S. (1993) *J. Biol. Chem. 268*, 16519−16527.
38. Rittinger, K., Divita, G., and Goody, R. S. (1995) *Proc. Natl. Acad. Sci. U.S.A. 92*, 8046−8049.
39. Huang, H., Chopra, R., Verdine, G. L., and Harrison, S. C. (1998) *Science 282*, 1669−1675.
40. Magnuson, V. L., Ally, D. S., Nylund, S. J., Karanjawala, Z. E., Rayman, J. B., Knapp, J. I., Lowe, A. L., Ghosh, S., and Collins, F. S. (1996) *BioTechniques 21*, 700−709.
41. Hu, G. (1993) *DNA Cell Biol. 12*, 763−770.
42. Moran, S., Ren, R. X., and Kool, E. T. (1997) *Proc. Natl. Acad. Sci. U.S.A. 94*, 10506−10511.
43. Eckert, K. A., and Kunkel, T. A. (1993) *Nucleic Acids Res. 21*, 5212−5220.
44. Mules, E. H., Uzun, O., and Gabriel, A. (1998) *J. Virol. 72*, 6490−6503.
45. Suo, Z., and Johnson, K. A. (1997) *Biochemistry 36*, 12459−12467.
46. Suo, Z., and Johnson, K. A. (1998) *J. Biol. Chem. 273*, 27259−27267.
47. Lanchy, J. M., Keith, G., Le Grice, S. F., Ehresmann, B., Ehresmann, C., and Marquet, R. (1998) *J. Biol. Chem. 273*, 24425−24432.
48. Furge, L. L., and Guengerich, F. P. (1999) *Biochemistry 38*, 4818−4825.
49. Jacobo-Molina, A., Ding, J., Nanni, R. G., Clark, A. D., Jr., Lu, X., Tantillo, C., Williams, R. L., Kamer, G., Ferris, A. L., Clark, P., Hizi, A., Hughes, S. H., and Arnold, E. (1993) *Proc. Natl. Acad. Sci. U.S.A. 90*, 6320−6324.
50. Sarafianos, S. G., Das, K., Tantillo, C., Clark, A. D., Jr., Ding, J., Whitcomb, J. M., Boyer, P. L., Hughes, S. H., and Arnold, E. (2001) *EMBO J. 20*, 1449−1461.

BI0160415